

PAPER • OPEN ACCESS

A new semi-empirical correlation for driving mass-flow rate calculation through ejectors for CO<sub>2</sub> heat pumps. Comparison with predictions of other methods.

To cite this article: G Boccardi *et al* 2020 *J. Phys.: Conf. Ser.* **1599** 012055

View the [article online](#) for updates and enhancements.



**ECS** **240th ECS Meeting**  
Digital Meeting, Oct 10-14, 2021  
**We are going fully digital!**  
Attendees register for free!  
**REGISTER NOW**

# A new semi-empirical correlation for driving mass-flow rate calculation through ejectors for CO<sub>2</sub> heat pumps. Comparison with predictions of other methods.

G Boccardi<sup>1</sup>, G Lillo<sup>2</sup>, R Mastrullo<sup>2</sup>, A W Mauro<sup>2</sup>, M Pieve<sup>1</sup> and R Trinchieri<sup>1</sup>

<sup>1</sup> Energy Department Production, Conversion and Use of Energy Division, Laboratory of Development of Chemical Processes and Thermofluidynamic, ENEA, C.R.Casaccia - Via Anguillarese 301, 00123 Roma (Italy)

<sup>2</sup> Department of Industrial Engineering, Federico II University of Naples, p.le Tecchio 80, 80125 Napoli (Italy)

Corresponding author e-mail: raniero.trinchieri@enea.it

**Abstract.** Carbon dioxide (CO<sub>2</sub>) is an interesting substitute of traditional HFCs in vapor compression systems, due to its environmentally friendly characteristics: zero ODP and extremely low GWP. Nevertheless, the use of CO<sub>2</sub> heat pumps in residential heating and cooling applications actually is still limited, due to the different operating conditions of gas cooling, they can perform significantly worse than conventional.

The use of ejection systems for the fluid expansion in a refrigeration cycle can contribute to recovery part of the mechanical energy otherwise dissipated as friction, leading to significant benefits in terms of performance. The ejector sizing is a critical point for the balancing of components and the correct operation of the CO<sub>2</sub> heat pump; in this regard, the availability of reliable methods for calculating the motive flow rate would be useful. In recent years, ENEA Laboratory DTE-PCU-SPCT of the Casaccia research center, along with the Industrial Engineering Department of Federico II University of Naples, carried on a project aimed at evaluating experimentally the effect of several ejectors geometries on the global performance of a CO<sub>2</sub> heat pump working with a transcritical cycle.

This paper presents a new semi-empirical correlation for the ejector primary mass flow rate calculation, developed by the experimental data, based on the hypothesis of isentropic and choked flow. The correlation is then tested on other experimental data available in the literature for different ejectors. Finally, the predictions are compared to others semi-empirical correlations present in the literature.

## 1. Introduction

The refrigeration and air conditioning sector contributes significantly to the direct and indirect greenhouse gas emissions. Systems efficiency influences indirect emissions while not eco-friendly refrigerants are the cause of direct emissions. Therefore, the growing international emphasis on global warming phenomena has moved the interest of the manufacturers as well as the scientific community to low-GWP refrigerants. The more promising alternatives as working fluids are the new synthetic fluids (such as hydrofluoroolefins, HFO fluids), fluids based on R32 as well as the natural fluids. The first two groups give good performance, but their slight flammability (ASHRAE A2L safety classification) is the main drawback that is limiting a wider diffusion. Among the natural fluids, the



use of CO<sub>2</sub> (GWP = 1), a nontoxic and non-flammable refrigerant, it is a viable alternative to synthetic refrigerants banned by the latest F-gas regulation [1].

The use of CO<sub>2</sub> as refrigerant in the sanitary hot water production is well known, as shown by

Neska et al. [2]. In particular, in case of water heating starting from low temperature, CO<sub>2</sub> shows high performance. Vice versa, the performance is not as good when CO<sub>2</sub> is used in air conditioning systems, as shown by Calabrese et al. [3]. Lower performances are primarily due to the throttling losses in the expansion process. In particular, higher water inlet temperature at gas cooler leads to higher exergetic throttling losses. The use of an ejector system as substitute of a conventional expansion valve can improve the performance of the overall system. Minetto et al. [4], through a numerical simulation, pointed out that the use of an ejector system can lead to a carbon dioxide heat pump performance comparable to that of R410A. Elbel et al. [5] and Lucas et al. [6] confirm that the use of the ejector improves the COP and exergy efficiency up to 17% in transcritical refrigeration cycle. In air conditioning systems, where the boundary conditions are variable, the multi-ejector system is preferable, as exposed by Banasiak et al. [7]. The COP improvements up to 7% as confirmed by experimental study of Haida et al. [8]. Moreover, Lawrence and Elbel [9] and Banasiak et al. [10] underline that the performance of an ejector cycle is strictly related to the performance of the ejector that is principally dependent on the proper design geometry, where the converging-diverging primary (motive) nozzle plays an important role.

In literature, some methods (Banasiak et al. [11], Lucas et al. [12]), and semi-empirical correlations (Banasiak and Hafner [7], Lucas et al. [12, 13], Martin et al. [14], Boccardi et al. [15]) for the calculations of the motive mass flow rate were found.

In this paper, the data obtained by some experimental campaigns conducted at ENEA's Casaccia Research Center on an air-to-water CO<sub>2</sub> heat pump, have been used for developing a new semi-empirical correlation to calculate the mass flow rate through ejectors based on the hypotheses of isentropic expansion and choked flow. Its performance are afterwards evaluated by means of a comparison between the literature correlations [7,13,15], also using some other experimental data available in the literature for different ejectors.

## 2. Literature survey on the previous methods and proposal of a new semi-empirical correlation

In a CO<sub>2</sub> heat pump, the ejectors usually operate with primary inlet pressures  $p_{in}$  higher than critical value  $p_{cr}$  (73.77 bar); moreover, the outlet pressures depend on the evaporator pressure and are usually lower than 40 bar.

According to the motive nozzle inlet temperature, the expansion process through the ejector can begin from two different thermodynamics conditions: supercritical state ( $T_{in} > T_{cr}$ ), or compressible liquid ( $T_{in} < T_{cr}$ ).

In supercritical state, the isentropic expansion proceeds in a different manner according to the inlet entropy value ( $s_{in}$ ); for instance, if  $s_{in} > s_{cr}$ , the thermodynamic state switches directly in superheated steam when the pressure drops below the critical pressure. Instead, if  $s_{in} < s_{cr}$ , the fluid switches in compressible liquid state when the temperature drops below the critical value: carrying on the expansion the fluid is in subcooled liquid state (when  $T_{in} < T_{cr}$ ) and after that in two-phase state when the saturation conditions are reached.

All the complex phenomena that happen during the expansion significantly influence the ejector performance. In this situation, it is reasonable to suppose that the motive flow is choked at the throat of the ejector driving nozzle (Banasiak [11], Lucas [12, 13], Martin [14]); consequently

- the ejector throat pressure  $p_{th}$  is equal to the  $p_{choked}$
- $p_{choked}$  and the motive mass flow rate only depend on the input conditions and on the complex phenomena that occur during the expansion till the choked conditions.

The complex flow conditions within the ejector make difficult to develop theoretical correlations to calculate the mass flow rate through ejectors; in particular, when the inlet conditions are supercritical, reliable theoretical methods for the calculation of choked mass flow rate are not available. However,

in the open literature, there are a few semi-empirical correlations based on experimental data and studies on calculation models to determine this process parameter.

Banasiak and Hafner [11], starting from a homogeneous equilibrium model proposed a new correlation that also takes into account the influence of the phase transition utilising a delayed equilibrium model [16]. The calculated critical mass flow with the correlation differ by up to 3% from the values measured in experimental tests on ejectors working in typical operating conditions of CO<sub>2</sub> heat pumps. Lucas et al. [12] present a numerical model based on homogeneous equilibrium approach and validate it with experimental data on ejectors working with and without the suction mass flow opened. The driving mass flux predictions were within an error margin of 10%.

Given the difficulty of having completely reliable models, semi-empirical correlations based on experimental data for component sizing are often used. Lucas et al. [13], suggest a semi-empirical method based on the data of an experimental campaign [6] on a multi-ejector heat pump using CO<sub>2</sub> as refrigerant. The method assumes isentropic flow and calculates the primary mass flow rate using the total energy equation:

$$G = S_{th} \cdot \rho_{th} \cdot u_{th} \quad (1)$$

The magnitudes in equation (1) were calculated assuming isentropic flow and as a function of the pressure at the throat ( $p_{th}$ ), supposed choked. This latter was empirically evaluated knowing inlet conditions and critical parameters as a function of some parameters experimentally determined.

Banasiak et al. [7] investigated the performance of a multi-ejector for CO<sub>2</sub> vapour compression units too; they proposed the following correlation for calculation of mass flow rate

$$G = \frac{\pi}{4} \phi^2 \left[ A \rho_{in}^2 + B \rho_{in} + C \frac{P_{in}^2}{P_{cr}} + D \frac{P_{in}}{P_{cr}} + E \right] \quad (2)$$

where  $A, B, C, D, E$  are coefficients adjusted for every ejector.

Boccardi et al. [15] proposed a correlation derived from the one proposed by Martin et al. [14], where a new geometric parameter was introduced to take into account the ejector geometries.

$$G = \phi^2 \frac{\pi}{4} k \left( A \left( \frac{P_{in}}{P_{cr}} \right)^B \left( \frac{\rho_{in}}{\rho_{cr}} \right)^C \left( \frac{T_{in}}{T_{cr}} \right)^D \left( \frac{L}{\phi_m} \right)^E + F \right) \quad (3)$$

In equation (3),  $A, B, C, D, E$  and  $F$  are parameters optimized to reach a minimal deviation between measurement and calculation.

In all the proposed correlations, the primary mass flow rate is a function only of the primary inlet conditions and critical parameters: this could be a limit for the calculation of the mass flow rate, which should be influenced by the non-transcritical expansion phase during flow till choked conditions.

For this reason, the correlation proposed in this article introduces some parameters for the overall expansion flow characterization. In particular, the liquid-two-phase transition point, which affects the achievement of sonic flow conditions, is defined.

The proposed correlation is inspired by those proposed by the ISO [17] for the sizing of valves and piping for gas/liquid two-phase flow:

$$G = k_d \cdot S_{th} \cdot G_t \quad (4)$$

In equation (4),  $k_d$  is the two-phase discharge factor, which is a function of geometry and flow conditions,  $S_{th}$  is the throat section area and  $G_t$  is the theoretical specific mass flow rate in an ideal

(isentropic) nozzle. The ISO procedure allows the calculation of  $G_t$  only when the initial state of the fluid is subcritical and it proposes different methods according to the initial thermodynamic state of the fluid. In the case of two-phase, saturated or slightly subcooled liquid inlet conditions,  $G_t$  is calculated as follow:

$$G_t = \sqrt{2\rho_{in}p_{in}} \sqrt{\frac{[-\omega \ln \eta - (\omega-1)(1-\eta)]}{(\omega(1/\eta - 1) + 1)}} \quad (5)$$

where  $\eta$  is ratio between the outlet and inlet pressures  $p_{out}/p_{in}$  and  $\omega$  is a characteristic parameter, function of the inlet conditions only. In choked conditions, in equation (5) the pressure ratio  $\eta$  is replaced by the choked pressure ratio  $\eta_{choked} = p_{choked}/p_{in}$  calculated as a function of  $\omega$ .

In high subcooled liquid inlet conditions, the saturation pressure at the initial temperature  $p_{sat}(T_{in})$  is assumed as  $p_{choked}$ , so  $\eta_{choked} = p_{sat}(T_{in})/p_{in}$ ,  $\omega \approx 0$  and the (5) becomes

$$G_t = \sqrt{2\rho_{in}(p_{in} - p_{out})} = \sqrt{2\rho_{in}p_{in}} \sqrt{1 - \eta_{choked}} \quad (6)$$

As mentioned above, it is not possible to directly apply the ISO when the inlet state is supercritical. On the other hand, in this case, the following considerations can be done:

- the motive flow surely is choked; consequently, the ejector throat pressure is equal to the sonic pressure and the mass flow rate only depends on the input conditions;
- the value of the choked parameters (pressure, velocity, etc.) depends on the starting point of the subcritical expansion phase, in turn depending on the supercritical starting point. For our experimental data, the starting point of subcritical expansion phase is highly subcooled or almost saturated, if an isentropic expansion is assumed;
- as mentioned above, in these situations, the ISO predicts  $\eta_{choked} = p_{sat}(T_{in})/p_{in}$  for high subcooling or uses the two-phase correlations for low  $\Delta T_{sub}$ ;
- for low  $\Delta T_{sub}$ , the sonic velocity is often reached at low vapour quality [18] and, therefore, with a low  $\Delta p$  respect to the saturation pressure  $p_{sat}(T_{in})$ .

For the reasons set out above, a saturation pressure  $p_{sat}(S_{in})$ , calculated considering an isentropic expansion from the initial conditions, is introduced in the correlation presented in this document for the mass flow rate calculation. This parameter can be considered closely related to  $p_{choked}$ .

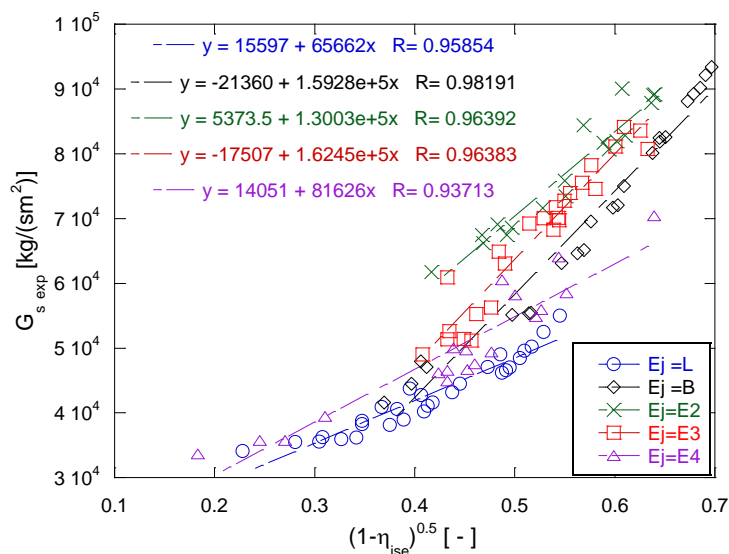


Figure 1. Specific mass flow rate  $G_s$  vs  $(1-\eta_{ise})^{0.5}$ .

In fact, figure 1 shows the experimental specific mass flow rate  $G_s$  as function of  $(1-\eta_{ise})^{0.5}$ , similar to the last term of correlation (6), where  $\eta_{ise} = p_{sat}(s_{in})/p_{in} \approx \eta_{choked}$ , for five ejectors, three of them (E2, E3, E4) tested by ENEA and the other two (B [11] and L [13]) by other researchers. The figure 1 highlights a dependence between  $G_s$  and  $(1-\eta_{ise})^{0.5}$  with a high coefficient of linear correlation.

In the proposed equation (7), in addition to the parameter  $(1-\eta_{ise})^{0.5}$ , three other parameters to describe the second expansion step till the sonic conditions, are introduced:

$$G = S_{th} \sqrt{2 \rho_{in} p_{in}} A (\sqrt{1 - \eta_{ise}})^B \left(\frac{p_{in}}{p_{tr}}\right)^C \left(\frac{\rho_{in}}{\rho_{tr}}\right)^D \left(\frac{T_{in}}{T_{tr}}\right)^E \left(\frac{p_{ise}}{p_{tr}}\right)^F \left(\frac{\rho_{ise}}{\rho_{tr}}\right)^G \left(\frac{T_{ise}}{T_{tr}}\right)^H \quad (7)$$

In (4),  $k_d$  is calculated as a function of the single phase discharge factors, depending on the geometry, which are experimentally estimated, and by  $\omega$ . Since for the ejector in study, the single phase discharge coefficients are not known, it was decided to not put geometric parameters in the proposed correlation and to proceed with the characterization of each ejector individually. The effect of varying the  $k_d$  with the operating conditions is therefore expressed by the variations of the other parameters.

### 3. Experimental setup and test procedure

The experimental data used in this paper were obtained testing a 30 kW CO<sub>2</sub> air-water heat pump in the experimental facility “Calorimetro Enea” at ENEA (Casaccia) research center, according to [19].

The heat pump (figure 2) was composed by a reciprocating semi-hermetic compressor (CP) driven by an inverter, a plate heat exchanger (GC), a finned coil (EVAP), an internal plate heat exchanger (IHE), an electronic valve (EEV), a multi-ejector expansion pack (EJEC) and a receiver, equipped with an oil recirculation loop driven by an on-off time-controlled valve (dashed line in figure 2).

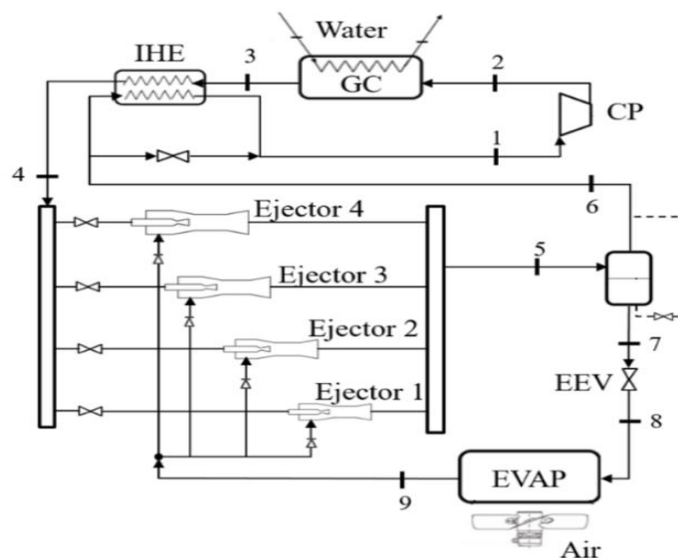


**Figure 2.** Layout of multi ejector CO<sub>2</sub> system.

During tests, ejectors 2, 3 and 4, of nozzle throat 1, 1.4 and 2 mm respectively, were separately activated by the heat pump control system. The heat pump was equipped with the instrumentation listed in table 1, which also shows the measurement range and uncertainties.

The boundary conditions in terms of air temperature, relative humidity, water temperature and mass flow rate were fixed and kept constant during the tests. In particular, the mass flow rate was measured placing the flow meter before the multi-ejector pack, thus on the primary flow. In addition, it was

possible to set the outlet evaporator and inlet compressor superheating by acting on the IHE bypass line through a modulating control valve. The trends of the thermodynamic measured variables were monitored via a software specifically designed. The main thermodynamic parameters were recorded and processed using Labview™ software.

**Table 1.** Measurement instrument and calibrated uncertainties

| Measurement                     | Range/Unit           | Uncertainty         |
|---------------------------------|----------------------|---------------------|
| Temperature (K-type)            | 0/150 °C             | ± 1.1 K             |
| Temperature (J-type)            | -40/80 °C            | ± 1.1 K             |
| Pressure                        | 0-60/0-100/0-160 bar | 0.08%               |
| Water volumetric flow rate      | 0/200 l/min          | 0.02% of reading    |
| Electrical power                | 0/25 kW              | Precision class 0.5 |
| CO <sub>2</sub> mass flow meter | 0/0.95 kg/s          | ± 0.10% of reading  |

All tests with ejector 2 were performed in subcritical conditions (ejector primary inlet temperature lower than critical temperature), whereas tests with ejector 3 and 4 were performed both in supercritical and subcritical conditions. Figure 3 shows the thermodynamics primary inlet conditions in the T-s diagram, divided by ejector.

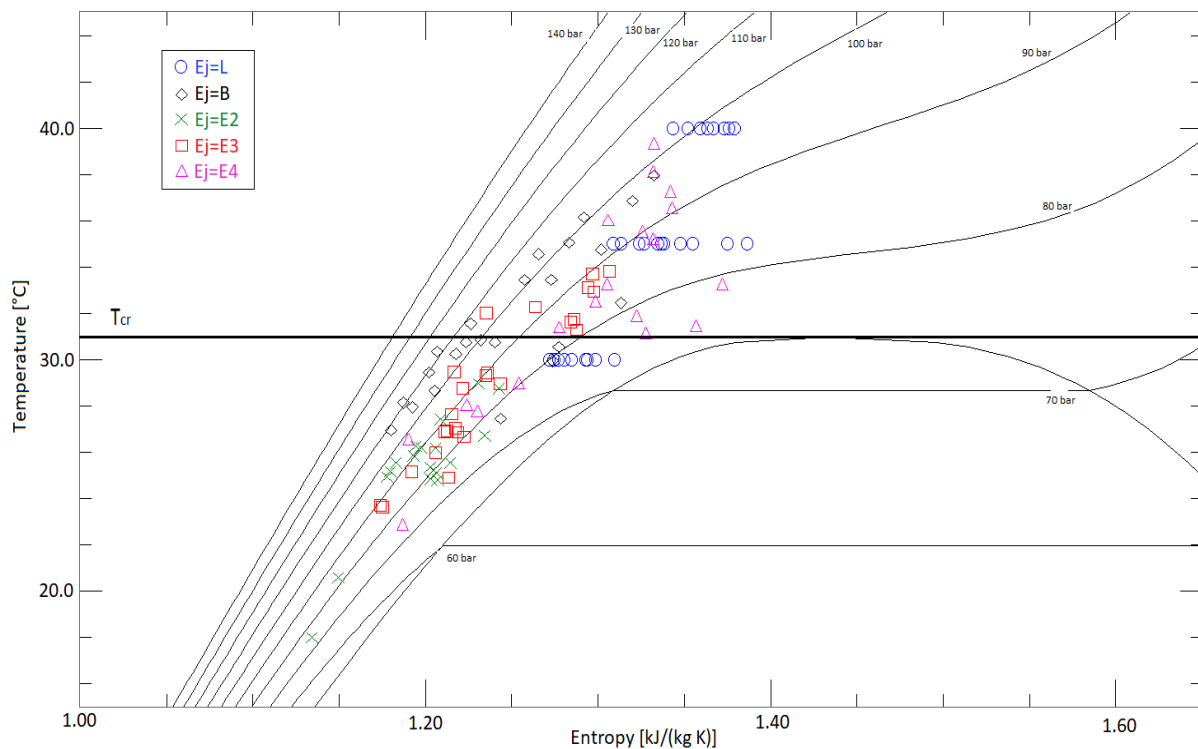


**Figure 3.** Test input conditions in the T-s diagram for the complete data set.

#### 4. Results and discussion

Firstly, the full data set composed by ENEA experimental data, obtained with ejectors E2, E3 and E4, having a similar geometry, and by Banasiak [11] and Lucas [13] data, on ejectors of different geometry, was defined. From this data set, data with  $p_{in} \leq p_{cr}$ ,  $s_{in} > s_{cr}$  and with primary inlet conditions too close to pseudocritical state were excluded. The main features of the used data are summarized in

table 2. It is worth noting that the nozzle length is considerably lower of 10mm, considered as the minimum relaxation length to have the onset of equilibrium flow: then non-equilibrium flow along the ejectors most likely have to be expected [20].

Secondly, using a mathematical solver (Labview, NI™), the data set was used to compute the optimum value for parameters present in the Lucas' procedure (to calculate  $p_{th}$  and, after this,  $\rho_{th}$  and  $u_{th}$ ) and in the equations (2), (3) and (7), able to minimize MSE for the specific mass flowrate calculation.

**Table 2.** Motive nozzle throat geometries and experimental test distribution (Total length calculated)

| Ejector<br>[#] | Nozzle<br>throat<br>$\phi$ (mm) | Nozzle<br>inlet |        | Nozzle<br>outlet |        | Total<br>Length<br>(mm) | Test            |                 |     |
|----------------|---------------------------------|-----------------|--------|------------------|--------|-------------------------|-----------------|-----------------|-----|
|                |                                 | $\phi$ (mm)     | degree | $\phi$ (mm)      | degree |                         | $T_{in}<T_{cr}$ | $T_{in}>T_{cr}$ | Tot |
| L[13]          | 0.62                            | *               | 45     | *                | *      | *                       | 10              | 19              | 29  |
| B[12]          | 0.91                            | 6               | 15     | 1.02             | 1      | 58.4                    | 13              | 10              | 23  |
| E2[15]         | 1.0                             | 3.8             | 30     | 1.12             | 2      | 32.1                    | 18              | 0               | 18  |
| E3[15]         | 1.4                             | 3.8             | 30     | 1.58             | 2      | 45.2                    | 19              | 6               | 25  |
| E4[15]         | 2.0                             | 3.8             | 30     | 2.24             | 2      | 64.1                    | 5               | 14              | 19  |

\* Data not available

In order to evaluate prediction performances of correlations, the parameter ER%, calculated by equation (8), has been introduced.

$$ER\% = \frac{G_{s\text{calc}} - G_{s\text{exp}}}{G_{s\text{exp}}} \quad (8)$$

Due to the very high error affecting the Lucas' procedure (ER% range  $-56 \div -26$  %), probably depending on the use of a specific semi-empirical correlation for the estimation of  $p_{th}$ , below only results of equations (2) and (3) and (7) are presented.

Figure 4 shows the percentage errors of the mass flow rate calculated by correlation (7) with respect to measured value, as a function of the ejector primary inlet entropy  $s_{in}$ . The predictions are good for every ejector: almost all the errors are in the range  $\pm 3\%$ . The figure 5 depicts the distribution of percentage errors for each ejector. The values are centred on  $ER\% = 0$ ; in particular, ejector B has the best performance with about 80% of errors in the range  $\pm 0.5\%$ .

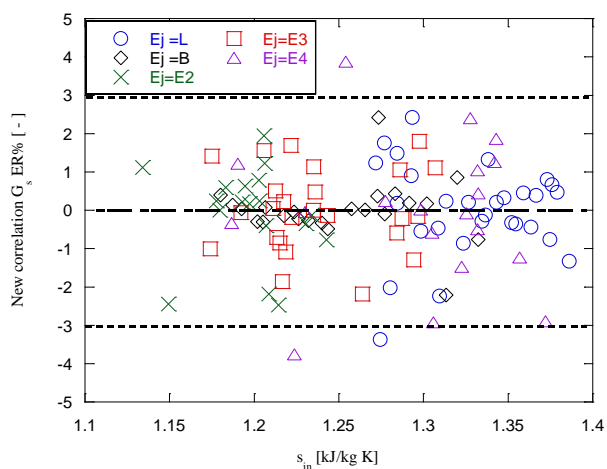


**Figure 4.** New correlation  $G_s$  error% vs  $s_{in}$ .

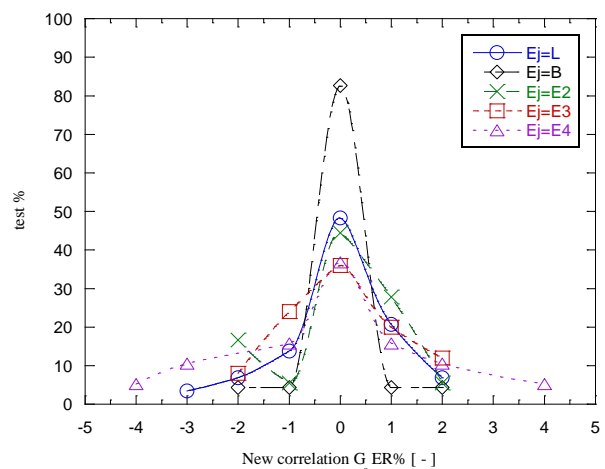


**Figure 5.** New correlation  $G_s$  error% distribution.

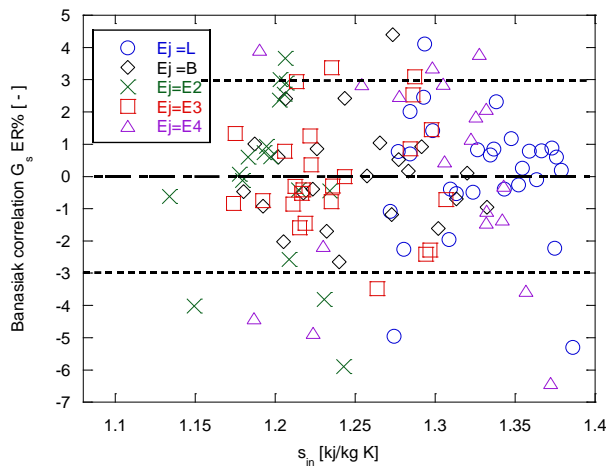


**Figure 6.** Banasiak correlation  $G_s$  error% vs  $s_{in}$ .

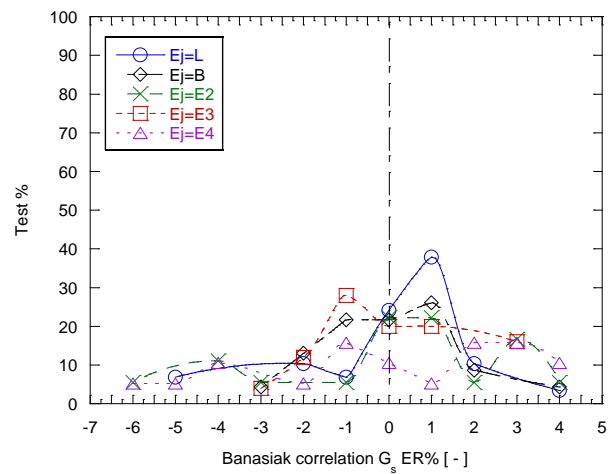


**Figure 7.** Banasiak correlation  $G_s$  error% distribution.

The mass flow rate percentage errors obtained with Banasiak equation remain interesting (figures 6 and 7), even if with greater errors and a wider and flat distribution range. Considering the individual ejectors, the predictions remain good enough for the ejector B, while the other ejectors have much more pronounced worsening of the MSE values.

**Table 3.** MSE [ $G_s$  (kg/s mm<sup>2</sup>)<sup>2</sup>] values for the correlation (7), (2) e (3)

| Correlation      | Ejectors |          |          |          |          |
|------------------|----------|----------|----------|----------|----------|
|                  | L        | B        | E2       | E3       | E4       |
| Banasiak (2)     | 5.89E-07 | 1.90E-07 | 3.60E-06 | 1.25E-06 | 2.41E-06 |
| Boccardi (3)     | 4.87E-07 | 2.82E-07 | 9.62E-07 | 8.45E-07 | 3.064-06 |
| New equation (7) | 2.34E-07 | 1.39E-07 | 8.80E-07 | 5.56E-07 | 8.90E-07 |

Performance of equation (2), (3) and (7) are summarized in table 3, where the MSE values calculated are displayed for each ejector.

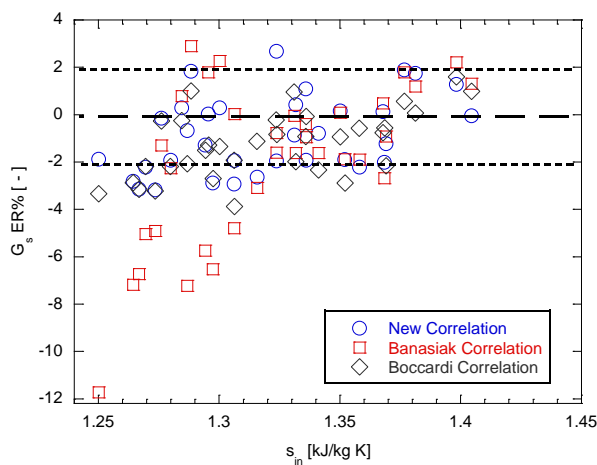


**Figure 8.** Correlation  $G_s$  error% vs  $s_{in}$  on Lucas Data Set [12].

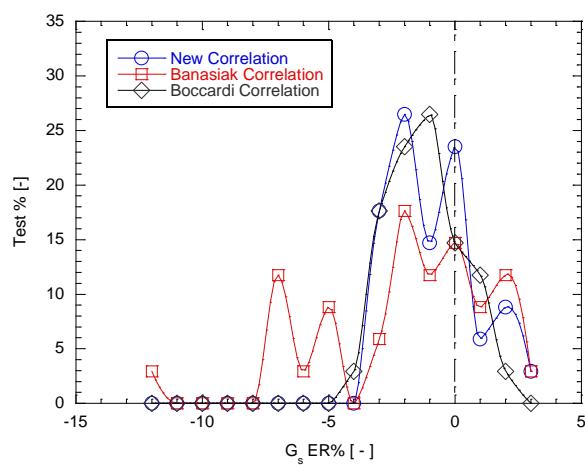


**Figure 9.** Correlation  $G_s$  error% distribution on Lucas Data Set [12].

To verify the performance of the correlations (2), (3) and (7) on data different from those used to calculate their coefficients, other experimental data available in the literature for the ejector L (Lucas et al. [12], tab. 2), were used. The correlations (2), (3) and (7) with the constants calculated using the initial data set were used to calculate the specific mass flow rate for the new experimental data. In figures 8 and 9 errors are compared between initial and verification data.

The new correlation has good performance, figure 8: the ER% range was between  $-3.2 \div 2.7$  with 73% of values between  $-2 \div 2\%$ . Figure 8 and 9 show a worsening of the predictions for the Banasiak correlation (3), especially for the low values of  $s_{in}$ ; the ER% range is  $-7.2 \div 2.9$  (with a point having  $ER\% = -11.7$ ) and, in particular, only 55% of ER% values are between  $-2 \div 2\%$ . The correlation (3) maintains good performance with a tendency to underestimate.

## 5. Conclusions

In order to improve the knowledge about ejector performance, new experimental data, in terms of motive nozzle mass flow rate, have been obtained during testing of a heat pump system with multi-ejector pack as expansion device. Transcritical motive nozzle inlet conditions, with pressure in the range  $74 \div 98$  bar, have been investigated.

The measured primary mass flow rate values have been elaborated with the mass flow rates calculated with using three existing semi-empirical correlations, Lucas et al. [13], Banasiak et al. and [7] Boccardi et al. [15], in order to find the best methods to assessing the motive nozzle mass flow rate. Moreover, a new semi-empirical correlation has been proposed and evaluated. We observed that:

- The performances of the correlations change as the geometry of the ejector changes: in particular, the MSE calculated on the specific mass flow rate of each correlation changes significantly with the variation of the ejector; with respect to the minimum value, tab. 3, it grows by about 6.4 times for equation (7), 18.9 for equation (2) and 10.9 for equation (3).
- the verification carried out on data not used [12] for the calculation of the correlation constants, showed a good reliability for the new semi-empirical equation (7).
- The new semi-empirical correlation, developing on the hypothesis of isentropic expansion and  $p_{choked} = p_{ise} = p_{sat}(s_{in})$ , has the best performance both for ENEA data than other data available in literature.

In conclusion, the correlation (7) showed very interesting performances for 5 ejectors geometries with the relative sets of experimental data, despite the lack of a geometric parameter that also takes into account the different flow conditions.

The objectives pursued in the future of the research will concern:

- The identification and study of phenomena occurring during expansion and their correlation with the evolving mass flow rate.
- The improvement of the new semi-empirical correlation with parameters that take into account the relationships between geometry and flow characteristics.
- The application of the correlations obtained for individual ejectors to calculate the flow rates of a multi-ejector CO<sub>2</sub> system having several ejectors working in parallel.

Moreover, it will be evaluated the possibility of identifying other methods and /or correlations to be used with reference to CO<sub>2</sub> input conditions.

**Nomenclature**

|                |                         |                          |
|----------------|-------------------------|--------------------------|
| S              | area                    | (m <sup>2</sup> )        |
| G              | mass flow rate          | (kg/s)                   |
| G <sub>s</sub> | specific mass flow rate | (kg/(s m <sup>2</sup> )) |
| k <sub>d</sub> | discharge coefficient   | (-)                      |
| L              | length                  | (m)                      |
| p              | pressure                | (bar)                    |
| s              | specific entropy        | (kJ/(kg K))              |
| T              | temperature             | (°C)                     |
| u              | velocity                | (m/s)                    |

**Greek letters**

|   |                    |                      |
|---|--------------------|----------------------|
| φ | diameter           | (m)                  |
| ρ | density            | (kg/m <sup>3</sup> ) |
| η | pressure ratio     | (-)                  |
| ω | ISO parameter [17] | (-)                  |

**Subscripts**

|      |                                   |
|------|-----------------------------------|
| calc | calculated                        |
| cr   | thermodynamic critical conditions |
| exp  | experimental                      |
| ise  | isentropic                        |
| in   | inlet                             |
| m    | average value                     |
| out  | outlet                            |
| sat  | saturation                        |
| t    | theoretical                       |
| th   | throat                            |
| sat  | saturation                        |
| sub  | subcooling                        |

**6. References**

- [1] Regulation (EU) No 517/2014 of the European Parliament and the Council of 16 April 2014 *Off. J. Union*
- [2] Neksa P, Rekstad H, Zakeri GR and Schiefloe PA 1998 CO<sub>2</sub>-heat pump water heater: characteristics, system design experimental results *Int J Refrig* **21** 172–9
- [3] Calabrese N, Mastrullo R, Mauro A W, Rovella P and Tammaro M 2015 Performance analysis of a rooftop, air-to-air heat pump working with CO<sub>2</sub> *Appl Therm Eng* **75** 1046–54
- [4] Minetto S, Cecchinato L, Brignoli R, Marinetti S and Rossetti A 2016 Water-side reversible CO<sub>2</sub> heat pump for residential application *Int J Refrig* **63** 237-50
- [5] Elbel S and Hrnjak P 2008 Experimental validation of a prototype ejector designed to reduce throttling losses encountered in transcritical R744 system operation *Int J Refrig* **31**(3) 411–22
- [6] Lucas C and Koehler J 2012 Experimental investigation of the COP improvement of a refrigeration cycle by use of an ejector *Int J Refrig* **35** (6) 1595-603
- [7] Banasiak K, Hafner A, Kriezi EE, Madsen KB, Birkelund M, Fredslund K and Olsson R 2015 Development and performance mapping of a multi-ejector expansion work recovery pack for R744 vapour compression units *Int J Refrig* **57** 265-76
- [8] Haida M, Banasiak K, Smolka J, Hafner A and Eikevik TM 2016 Experimental analysis of the R744 vapour compression rack equipped with the multi-ejector expansion work recovery module *Int J Refrig* **64** 93-107
- [9] Lawrence N and Elbel S 2015 Analysis of two-phase ejector performance metrics and comparison of R134a and CO<sub>2</sub> ejector performance *Sci Technol Built En* **21** (5) 515-25
- [10] Banasiak K, Hafner A and Andresen T 2012 Experimental and numerical investigation of the influence of the two-phase ejector geometry on the performance of the R744 heat pump *Int J Refrig* **35** (6) 1617–25
- [11] Banasiak K and Hafner A 2013 Mathematical modelling of supersonic two-phase R744 flows through converging-diverging nozzles: The effects of phase transition models *Appl Therm Eng* **51** 635-43
- [12] Lucas C, Rusche H, Schroeder A and Koehler J 2014 Numerical investigation of a two-phase CO<sub>2</sub> ejector *Int J Refrig* **43** 154-66

- [13] Lucas C, Koehler J, Schroeder A and Tischendorf C 2013 Experimentally validated CO<sub>2</sub> ejector operation characteristic used in a numerical investigation of ejector cycle *Int J Refrig* **36** (3) 881-91
- [14] Martin K, Rieberer R and Hager J 2006 Modeling of Short Tube Orifices for CO<sub>2</sub> *Int Refrig. and Air Conditioning Conference*. Paper 781 <http://docs.lib.purdue.edu/iracc/781>
- [15] Boccardi G, Lillo G, Mastrullo R, Mauro A W, Saraceno L, Pieve M and Trinchieri R 2017 Experimental investigation on predictive models for motive flow calculation through ejectors for transcritical CO<sub>2</sub> heat pumps *J Phys: Conf. Ser* **923** 012018
- [16] Attuo A and Seynhaeve JM 1999 Steady-state critical two-phase flashing flow with possible multiple choking phenomenon. Part 1: physical modelling and numerical procedure *J Loss Prevent Proc* **12** 335-45
- [17] ISO/DIS4126-10 2008 Safety devices for protection against excessive pressure – Part 10: Sizing of safety valves for gas/liquid two-phase flow
- [18] Chung M S, Park S B and Lee H K 2004 Sound speed criterion for two-phase critical flow *J sound vib* **276** 13-26
- [19] UNI EN 14511-3 2011 Air conditioners, liquid chilling packages and heat pumps with electrically driven compressors for space heating and cooling. Part 3: Test methods
- [20] Fisher H G, Muller A R, Forrest H S, Noronha J A, Grossel S S, Shaw D A, Huff J E and Tilley B J 1992 *Emergency Relief System Design Using DIERS Technology* (New York, The Design Institute for Emergency Relief Systems of the American Institute of Chemical Engineers)